The NOMAD Experiment : Status Report

Marco Laveder[a] *

[a]Dipartimento di Fisica " G.Galilei", University of Padova and
INFN Sezione di Padova, I-35131 Padova, Italy

The NOMAD experiment has been designed to search for ν_τ appearance in the CERN wide-band neutrino beam . The detector is now completed and has been further improved. All subdetectors are working well. The experiment, where the search for oscillation is based on kinematical criteria, will reach the sensitivity $\Delta m^2 > 0.7$ eV^2 for maximal mixing and $\Delta m^2 > 50$ eV^2 for mixing angles $\sin^2 2\theta > 3.8 \times 10^{-4}$ after 2 years of running, making possible to explore a region of cosmological interest. Preliminary measurements are presented from the 1994 and 1995 data samples.

1. Introduction

The goal of the NOMAD experiment [1] are neutrino oscillations $\nu_\mu \to \nu_\tau$. The experiment searches for the appearance of tau neutrinos ,ν_τ, in the CERN SPS wide band neutrino beam, which consists mostly of muon neutrinos ν_μ . It is therefore an appearance experiment. The search is based on the detection of τ^-production and decay:

$$\begin{aligned} \nu_\tau + N \quad &\to \quad X + \tau^- \\ &\qquad \tau^- \quad \to \quad \tau^- decay\ mode \end{aligned}$$

The natural contamination of ν_τ in the SPS neutrino beam is negligible ($\simeq 10^{-7}$),therefore τ^-eventually observed could only result from $\nu_\mu \to \nu_\tau$ or $\nu_e \to \nu_\tau$ oscillations.

Neutrino oscillations can take place if the states of the neutrinos produced in the weak interaction processes are not stationary, but rather are superpositions of stationary states of neutrinos having different nonzero masses .

For massive ν , the flavour eigenstates ν_e ,ν_μ , ν_τ , can be expressed in terms of the mass eigenstates ν_1 , ν_2 , ν_3 , through an unitary mixing matrix.

In the simplified hypothesis of a mixing between two neutrino families, the probability of observing $\nu_\mu \to \nu_\tau$ oscillations at a distance L is given by

$$P = \sin^2 2\theta \sin^2 1.27 \frac{\Delta m^2 (eV^2) L(km)}{E_\nu (GeV)} \tag{1}$$

where E_ν is the neutrino energy in GeV ,θ the mixing angle, $\Delta m^2 =\mid m_1^2 - m_2^2 \mid$ the eigenstates mass squared difference in eV^2 and L is the distance in Km between the neutrino production and observation.

After two years of running ,equivalent to an integral of 2.4×10^{19} protons-on-target (pot), a sample of about 1.5 million neutrino interactions will be collected within NOMAD active target. The analysis of these events will allow probing neutrino oscillations in a wide region of the parameter space ($\sin^2 2\theta, \Delta m^2$), see Fig. 1, exploring a mass region of cosmological interest :

$m_{\nu_\tau} \geq 0.8$ eV for $\sin^2 2\theta = 1$.
$m_{\nu_\tau} \geq 7.0$ eV for $\sin^2 2\theta \geq 3.8 \times 10^{-4}$.

In fact if tau neutrinos have a mass in the region of 10 eV, they are suitable candidates for hot dark matter .

While the existence of the tau neutrino in this mass region was already investigated by previous experiments (see for example Refs[5–8]), NOMAD improves the most stringent limit given by the E531 exp. [5] by one order of magnitude.

2. The neutrino beam

The CERN SPS neutrino Wide Band Beam (WBB) is produced using 450 GeV protons hitting a Be target with a cycle of 14.4 s. The intensity delivered is about 2×10^{13} protons per cycle.

The NOMAD detector is located downstream

*Presented on behalf of the NOMAD Collaboration.

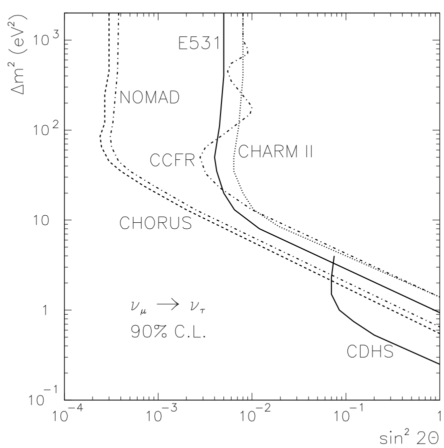

Figure 1. Existing limits in the neutrino oscillation parameter space[5–8] compared to the one achievable by on-going experiments[1, 4] after two years of running.

the target at about 820 m . The relative abundances of the different species of neutrinos and their average energies are listed in Table 1.

The sensitivity of the experiment is calculated for an integrated intensity of 2.4×10^{19} pot which corresponds to about: 1.1×10^6 ν_μ CC events, 3.7×10^5 ν_μ NC events and 1.3×10^4 ν_e CC events in the fiducial target of the NOMAD detector (mass = 2.7 tons, area = 2.6×2.6 m^2).

3. Neutrino tau search

NOMAD aims at identifying τ^-production and decay using suitable kinematical selection criteria such as missing P_T, angular correlations etc. To do so, very good energy, momentum and angular resolution are needed. The $\tau^-$is detected through a large variety of its decay modes listed in Table 2. As an example of the kinematical analysis the electronic decay of τ^-will be considered. The background to this channel is caused by ν_e charged current events which constitute $\approx 1\%$ of the total number of neutrino interactions.

Table 1
CERN WBB averaged neutrino energies

Neutrino	$< E_\nu > (GeV)$	r.a.
ν_μ	26.9	1.0
$\bar{\nu}_\mu$	21.7	0.06
ν_e	47.9	0.007
$\bar{\nu}_e$	35.3	0.002

Table 2
Summary of detection channels

τ^- decay mode	Br (%)
$e^-\nu_e\nu_\tau$	18.0
$\mu^-\nu_\mu\nu_\tau$	17.6
$\pi^-\nu_\tau$	11.7
$\rho^-(2\pi)\nu_\tau$	25.2
$a_1^-(3\pi)\nu_\tau + n\pi^0$	14.4
Total	86.9

For each event the sum of the momenta transverse to the beam direction ,P_T, for all seen particles is calculated and a resulting missing P_T vector (P_T^m) is reconstructed. The angles ϕ_{eh} between the electron momentum and the momentum of hadrons and ϕ_{mh} between $P_T^m$and the hadron vector are defined in the plane perpendicular to the beam direction as shown in Fig. 2 (a,b). In the case of $\nu_e CC$ background simulations show that the angle ϕ_{eh} is sharply peaked at π (Fig. 2 (c)). On the contrary for ν_τ interactions, the τ^- lepton balances the hadrons, while the electron from τ^-decay acquires a finite P_T relative to the τ^- direction and will not be back–to–back with the hadron vector (Fig. 2 (d)). So while the P_T^min the genuine ν_τ interactions is due to the missing of the two ν_e and $\nu_\tau\tau^-$decay neutrinos and therefore is along the τ^-direction with a peak near π (Fig. 2 (f)), P_T^m in the $\nu_e CC$ events is expected to arise either from missed neutral particles, such as neutrons and K_L^0, which contribute to an enhancement in ϕ_{mh} near 0, or from mismeasurements which will give a flat contribution to ϕ_{mh} (Fig. 2 (e)). It is than expected that the ϕ_{eh} and ϕ_{mh} distributions are

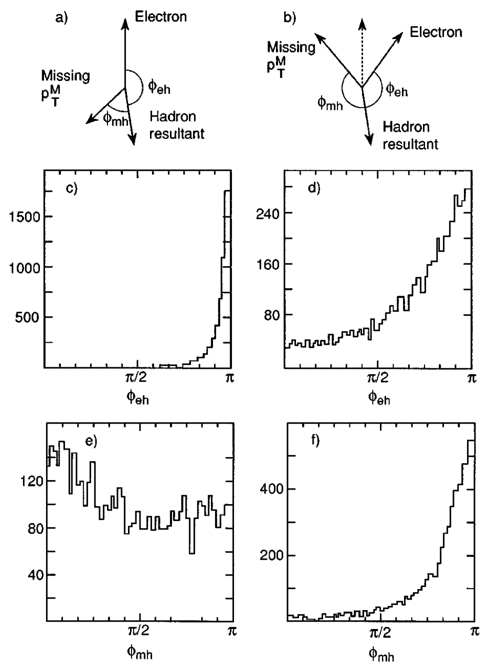

Figure 2. Kinematic variables used in the oscillation search for a) ν_e CC b) ν_τ CC; $\tau \rightarrow e$ in the plane orthogonal to the incident ν. MC distribution of ϕ_{eh} for c) background d) signal. MC distribution of ϕ_{mh} for e) background f) signal. See text for the definition of angles.

quite different for the signal ($\nu_\tau CC$) and the background ($\nu_e\, CC$) events. Similar distributions are used in the muonic and hadronic decay channels of the τ^- to select the signal. A two dimensional cut in the plane (ϕ_{eh}, ϕ_{mh}) is then defined and the contamination from all background sources, e^- background coming from $\nu_e\, CC$ and e^- background coming from the hadronic jet in $\nu_\mu\, NC$,remaining after all selection cuts is minimized. It was evaluated that for an efficiency for the signal of 13.5% one expects 4.6 background events in total. It is important to stress that most of the backgrounds can be studied in the data themselves rather than having to be estimated from Monte Carlo. The e^- background coming from the hadronic jet in $\nu_\mu\, NC$ can be studied using $\nu_\mu\, CC$ events and ignoring the μ . The background coming from $\nu_e\, CC$ can be studied replacing the μ in $\nu_\mu\, CC$ events with a simulated e^-.

4. Detector performance

The NOMAD detector measures and identifies the electrons, muons, photons and hadrons produced in neutrino interactions. A reconstructed charged current candidate (1995 run) is shown in fig. 3. A detailed description of the detector

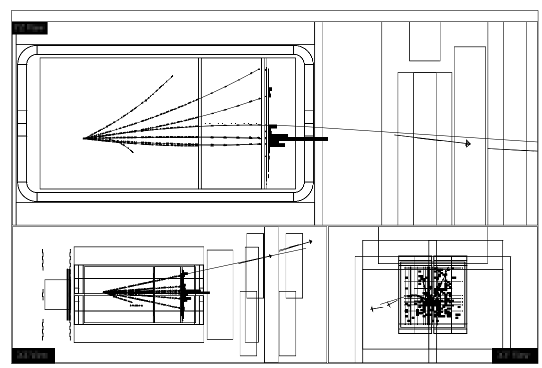

Figure 3. A reconstructed charged current candidate (1995 run)

is given elsewhere[2]. The active target consists of drift chambers (DC) with low average density ($\approx$ 0.1 g/cm^3). The measured single hit resolution is 180 μm. These DC are located in a magnetic field of 0.4 T which allows the determination of the momenta of charged particles with little degradation due to multiple scattering, given the low Z of the chamber material: $\sigma_p/p \approx 5\%/\sqrt{L} \oplus 0.8\% p/\sqrt{L^5}$ (L in m, p in GeV/c). The active target is followed by a transition radiation detector (TRD) to tag electrons, a preshower (PS) detector, an electromagnetic calorimeter (ECAL,$\sigma(E)/E \approx 4\%/\sqrt{E/GeV}$ for electrons) a muon absorber and muon chambers.

In the 1994 run all these detectors were functional, but only two out of eleven drift chamber target modules were installed behind a provisional nonactive target. More drift chambers were installed gradually for the 1995 run, and the detector was completed in August 1995 . In the beginning of 1995 a hadronic calorimeter[3] (HCAL,$\sigma(E)/E \approx 120\%/\sqrt{E/GeV}$) was installed downstream of the ECAL and a front calorimeter was implemented upstream of the active target.

5. Particle identification

Several detectors contribute to electron identification. The TRD achieves a pion rejection of 10^{-3} whith an electron efficiency $> 90\%$ for $p > 2$ GeV/c as measured in test beams. Consistency of the momentum measured in the drift chambers with the energy and shower shape measured by the ECAL/PS system yields an additional rejection factor ≥ 100.

Fig. 4 shows the evolution of this consistency variable after successive cuts. We interpret the peak near zero as electrons originating from photon conversions and ν_e CC interactions.

The low density NOMAD target (about 1.3 X_0 in total) allows the detection of photons and π^0 in the ECAL/PS system with a good spatial and energy resolution . Gamma candidates were selected with the following criteria: i) energy larger than 200 MeV; ii) no DC tracks pointing to the cluster (within 15 cm); iii) a pre-shower signal higher than 4 mip and matched to the cluster closer than 6 cm ; iv) less than 4 gamma candidates per event; v) reconstructed vertex inside the fiducial volume.

A clear π^0 peak is observed in the measured two photon invariant mass distribution (Fig. 5) from a sample of 1995 data.

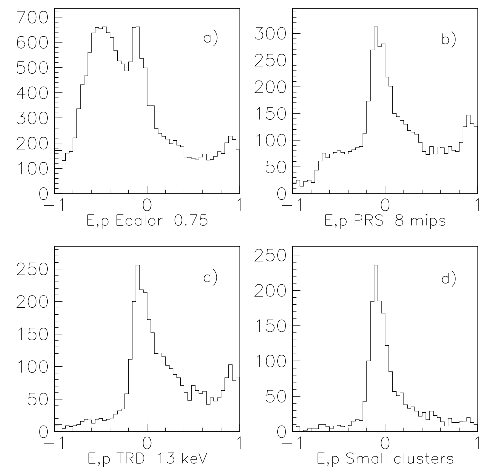

Figure 4. The distribution of $(E-p)/(E+p)$ for a) all drift chamber tracks which point to a cluster in ECAL with energy greater than 0.75 GeV; b) same with cut on the preshower energy; c) same with TRD pulse height cut; d) same with cut on the size of the ECAL cluster.

Charged hadrons appear as tracks in the drift chambers which are neither identified as a muon nor as an electron. The measured hadron momentum and multiplicity distributions agree reasonably well with Monte Carlo predictions.

Muons are identified by drift chamber tracks matching the corresponding tracks in the muon chambers. As expected, the measured muon momentum spectrum is dominated by negative muons from charged current neutrino interactions (Fig. 6). The contribution of positive muons is the one expected according to the beam contamination. The distribution in momentum is in agreement with the MC prediction based on the ν flux energy distribution.

6. Conclusion

The NOMAD detector is working well. The active target was fully completed in August 1995. Electrons and muons have been identified and distinguished from charged hadrons. π^0's have also been identified. NOMAD will continue taking data until the end of 1997 to search for $\nu_\mu \to \nu_\tau$ oscillations.

Acknowledgments

Thanks are due to the NOMAD technical staffs for their invaluable support.

I wish to thank the organizers for this very interesting and fruitful workshop in the nice historic city of Toledo.

REFERENCES

1 NOMAD proposal and addenda, CERN-SPSLC/91-21, CERN-SPSLC/91-48, CERN-SPSLC/91-53, CERN-SPSLC/93-19, CERN-SPSLC/94-21, CERN-SPSLC/94-28.

2 A. Rubbia, NOMAD Status Report, *Nucl. Phys.* **B** (Proc. Suppl.) **40** (1995) 93.

3 NOMAD Collab., CERN-SPSLC/93-31.

4 CHORUS proposal, CERN-SPSLC/90-42, CHORUS Collab., M. de Jong et. al., CERN-PPE/93-131.

5 N. Ushida et al., *Phys. Rev. Lett.* **57** (1986) 2897.

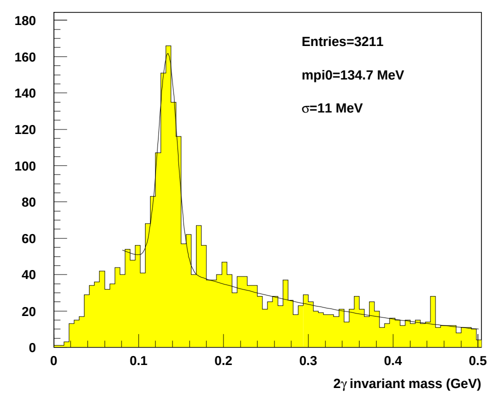

Figure 5. Two photon invariant mass distribution in NOMAD ECAL/PS system.

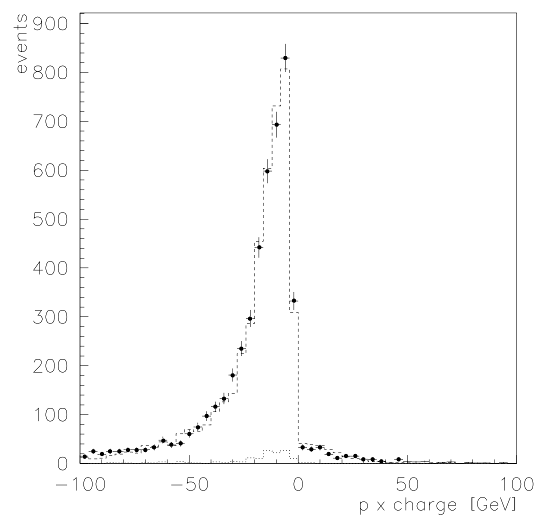

Figure 6. Momentum distribution for both negative and positive muons originating from the in-active target (1994 data). The measured data points are compared to the Monte Carlo prediction (dashed line).

6 CDHS Collab., F. Dydak et. al., *Phys. Lett.* **B134** (1984) 281.
7 CHARM-II Collab., M. Gruwe et. al., *Phys. Lett.* **B309** (1993) 46.
8 CCFR Collab., K.S. McFarland et al. in Proceedings of Intern. Europhysics Conf. on H.E.P., Brussels 1995, (in press).